J_ID: JTE DOI: 10.1520/JTE20150186 Date: 21-June-16 Stage: Page: 1 Total Pages: 11

PROOF COPY [JTE20150186]

Journal of Testing and Evaluation

doi:10.1520/JTE20150186 / Vol. 45 / No. 4 / July 2017 / available online at www.astm.org

D. Kocsis,[1] G. Deák,[2] S. Kéki,[3] Z. A. Godó,[4] and R. Horváth[5] AQ1

Creep and Quasi-Relaxation Examination of Artificially Aged Plasticized PVC

Reference

Kocsis, D., Deák, G., Kéki, S., Godó, Z. A., and Horváth, R., "Creep and Quasi-Relaxation Examination of Artificially Aged Plasticized PVC," *Journal of Testing and Evaluation*, Vol. 45, No. 4, 2017, pp. 1–9, doi:10.1520/JTE20150186. ISSN 0090-3973

Manuscript received May 5, 2015; accepted for publication May 4, 2016; published online xx xx xxxx.

[1] Dept. of Chemical and Environmental Engineering, University of Debrecen, 2-4 Ótemető St., Debrecen HU-4028, Hungary (Corresponding author), e-mail: kocsis.denes@eng.unideb.hu

[2] Dept. of Applied Chemistry, Univ. of Debrecen, 1 Egyetem Square, Debrecen HU-4032, Hungary, e-mail: deak.gyorgy@science.unideb.hu

[3] Dept. of Applied Chemistry, Univ. of Debrecen, 1 Egyetem Square, Debrecen HU-4032, Hungary, e-mail: keki.sandor@science.unideb.hu

[4] Dept. of Information Technology, Univ. of Debrecen, 26 Kassai St., Debrecen HU-4028, Hungary, e-mail: godo.zoltan@inf.unideb.hu

[5] Dept. of Chemical and Environmental Engineering, Univ. of Debrecen, 2-4 Ótemető St., Debrecen HU-4028, Hungary, e-mail: horobjan@gmail.com

ABSTRACT

This paper introduces long-term tensile and quasi-relaxation tests of polyvinylchloride (PVC) fibers. During creep, the longitudinal and cross-sectional changes were measured of unaged and aged PVC fibers loaded with the same weight. In the quasi-relaxation section, where deformation was frozen, the stress changes were determined. During the examination of the creep, the Poynting–Thomson model described the phenomenon with sufficient accuracy (min R^2 0.9628) and the calculated parameter values characterized the aging process well. In the relaxed phase, the Poynting–Thomson model was not adequate, and, therefore, the second-order time derivatives were also involved in the applied model. Aging significantly resulted in parameter changes in this section as well.

Keywords

aging, creep, material property tests, PVC, relaxation

Introduction

The plastic products (heating pipes, tubes, barrier films, etc.) are typically planned for a long service life. Sometimes unexpected degradation events happen long before the end of the planned lifecycle (gas pipes crack, thermal water pipelines fracture, etc.). This can be the consequences of the degradation of plastics under external effects. Extensive knowledge of polymer degradation is required by many industrial applications [1]. The fate of outdoor aged polymers can be anticipated from accelerated laboratory tests; therefore, artificial aging experiments of plastics are considered to be important.

A number of material models try to describe the material behavior, from simple rheological models (Hooke, Newton, St. Venant) to complex material models. These can be formed as a combination of the simple models (e.g., Maxwell, Poynting –Thomson, Burgers). More sophisticated constitutive material models exist with the modification of the previous ones taking into account physical aspects of material internal dissipation [2,3]. This more precisely describes the material behavior, such as creep, relaxation, inertia, etc. Based on these models, exploring can be used for describing the material behavior accurately. In this case, this is done by determining its characteristic material parameters. Another aim is to identify the parameter changes caused by artificial aging, and to obtain information about their changing direction and magnitude.

The thermoplastic materials at small deformation behave as visco-elastic, and visco-plastic at high deformation. For the simulation of their behavior, a proper material model is necessary. There are widely used practical solutions for the simulation of thermoplastic materials, which are based on modifications to metal-based models. These models try to predict the behavior of thermoplastics. One is the semi-analytical model for polymers (SAMP) model introduced by Haufe et al. [4]. It considers the hydrostatic pressure dependence of thermoplastics' yield stress. Experimental studies are often based on modeling the creep and the stress relaxation together [5].

Recently, several material models have been formed. They try to predict the material behavior of thermoplastics by splitting the overall stress into different parts. In many cases, these models work with a different number of material parameters, such as those created by Krempl and Ho [6] for PA66 nylon, which had 15 parameters. Similar models were formed for high density polyethylene (HDPE) [7], polyoxymethylene (POM) [8], and polypropylene (PP) [9]. Nikolov and Doghri [10] presented a micromechanically based constitutive model for the small deformation behavior of HDPE. A method for modeling the nonlinear viscoelastic response of polymers was introduced by Joseph [11], with the comparison of model response and experimental data of different materials including polyvinylchloride (PVC). Pagnacco et al. [2] proposed a hybrid numerical/experimental approach to determine elasticity and viscoelasticity parameters of an isotropic material, and they demonstrated an application to a real rigid PVC plate. It is obvious that choosing the right number of parameters for an appropriate description of a material behavior is crucial. Yonan et al. [12] presented a nonlinear visco-plastic material model for PVC; a total of seven material parameters are necessary.

Numerous authors used fractional calculus for describing the properties of viscoelastic materials. Nonnenmacher and Glöckle [13] generalized the Poynting–Thomson model by applying the fractional calculus. Gloeckle and Nonnenmacher [14] presented an exactly solvable fractional model of linear viscoelastic behavior. Metzler and Nonnenmacher [15] investigated fractional relaxation processes and applied fractional rheological models for the description of viscoelastic materials. Mainardi and Spada [16] provided an overall survey to the viscoelastic models constructed via fractional calculus. Liu and Xu [17] applied constitutive equations of viscoelastic materials involving three different fractional parameters. They presented the calculated material parameter values for the experimental data of a viscoelastic material.

With regard to the known beneficial properties of PVC, a number of earlier studies examined the property changes caused by different aging processes. The most important factors influencing degradation of PVC materials include oxygen, humidity, mechanical stress, aggressive media, and ionizing radiation, all being accelerated by increasing temperature [18]. PVC exposed to weathering deteriorates and becomes increasingly colored and brittle. This results in a continuous decrease in mechanical properties such as tensile strength, elasticity, and impact resistance [19]. Artificial aging is usually performed at a high temperature, such as Yarahmadi et al. [20]. They studied the effects of heat treatment on the mechanical properties of PVC. Zhou et al. [21] investigated the creep performance of PVC aged at high temperature. Barbero and Ford [22] examined physical aging and temperature effects on PVC creep and relaxation. They applied the equivalent time temperature method to deal with long-term creep data. In addition, many studies work with photodegradation tests, including Ito and Nagai [23] and D'Aquino et al. [24]. D'Aquino uses a simplified mathematical model to predict PVC photodegradation.

The aim of this work is to investigate and describe the behavior of the examined material with sufficient precision using the applied load at constant temperature, and to gain information about the aging process using this model. Therefore, this work tries to minimize the number of necessary material parameters, which are used to characterize the possible changes and the level of degradation.

Experimental

TEST MATERIAL

Soft PVC fibers were used in the measurements, which were extruded from LE 411 type granulate produced by BorsodChem (Kazincbarcika, Hungary). Material composition is S-5070 PVC ($K = 70$) 60.30 wt. %; Bis(2-ethylhexyl) phthalate 37.39 wt. %; TM181-FSM stabilizer 0.90 wt. %; MMA/EA 1.21 wt. %; E-wax 0.18 wt. %; and Uvitex OB fluorescent whitener 0.02 wt. %. Mechanical properties are hardness shore A 72; density 1.217 g/cm^3; tensile strength 18.1 MPa; and elongation at break 340 %. The diameters of the fibers were approximately 8 mm, and the examined length was 250 mm.

INSTRUMENTS

The PVC fibers were exposed to UV light from Sylvania ultraviolet G30W lamps (two lamps, ultraviolet radiation with a peak at 253.7 nm, illumination intensity: 2×1720 mW/cm^2, and the distance between the UV light and the PVC material:

J_ID: JTE DOI: 10.1520/JTE20150186 Date: 21-June-16 Stage: Page: 3 Total Pages: 11
PROOF COPY [JTE20150186]

FIG. 1 Schematic view of the experimental system: (a) stretched PVC fiber, (b) load cell, (c) weight loaded on the specimen, and (d) pulley.

25 cm). The measurements were carried out both on unaged and aged specimens. Two different series of aging took part: 2541 h long and 4000 h long. Three specimens were examined in each case. For the tests, a Rinstrum N320 type load cell (capacity: 5000 N) was used. The longitudinal and transverse values were determined by a caliper and a micrometer.

TECHNICAL EXECUTION OF TESTS

During the experiment, the fibers were pulled out over a table with one end fixed to the load cell. The other end was run over a pulley and it was loaded with an attached weight (50 N) when the tests was initiated. The role of temperature is very important as it significantly influences the behavior of thermoplastic polymers [25]. The temperature was 295.65 ± 0.5 K during the tests; thus, it is considered to be almost constant. Marking was performed on the specimens and the baseline values were recorded. Change was measured to determine the longitudinal deformation, and diameter was measured for transverse change. The load was the same in each case, and from its nature it is considered to be an infinite fast loading. The experimental system can be seen in **Figs. 1** and **2**.

FIG. 2 Pictures of the experimental system.

The weight loading of the specimen moved vertically downward. In each case during this experiment, the weighted end was stopped by placing blocks under it after a three-and-a-half hour creep period. Thanks to this "setup," the further longitudinal deformation was frozen. Then quasi-relaxation (not based on standards like ASTM E328-13, ASTM D6048-07, etc.; hereinafter named simply relaxation) was studied based on the load cell's values and the longitudinal and transverse deformation. AQ2 Finally, after removing the weight, the specimen was removed from the table in an idle state. The length and diameter were measured again at different times. Thus, the following stages can be examined during and after the experiment (**Table 1**).

Results and Discussion

The examinations are based on the deviatoric and spherical split, which is recently applied by several authors [12,26,27]. The split of the stress tensor and deformation tensor can be seen in the Appendix. A universal model introduced by Asszonyi et al. [28] consists of the Poynting–Thomson body with an additional inertial element. The authors called the resulting model the Kluitenberg–Verhás body, which can be written after splitting:

$$\boldsymbol{\sigma}^d + \tau^d \dot{\boldsymbol{\sigma}}^d = \alpha^d \boldsymbol{\varepsilon}^d + \beta^d \dot{\boldsymbol{\varepsilon}}^d + \gamma^d \ddot{\boldsymbol{\varepsilon}}^d \quad (1)$$

$$\boldsymbol{\sigma}^s + \tau^s \dot{\boldsymbol{\sigma}}^s = \alpha^s \boldsymbol{\varepsilon}^s + \beta^s \dot{\boldsymbol{\varepsilon}}^s + \gamma^s \ddot{\boldsymbol{\varepsilon}}^s \quad (2)$$

It is apparent that, in this case, the stress first derivative and deformation first and second derivative are included in the equations. The following examines whether these parameters are sufficient in number for the studied case.

Deviatoric and spherical split is applied, because in terms of viscoelasticity the deviatoric and spherical parts behave independently based on general mechanical–thermodynamical considerations [28]. For example, in the case of a uniaxial process, the complex, multi-parametric viscoelastic behavior of tensile strength and deformation can be divided into two simpler, less parametric behaviors. This split makes the fitting of the material coefficients from experimental data much easier. Therefore, it is advantageous both from a theoretical and an evaluating perspective. The investigation is continued with the analysis of the deviatoric part. The creep and quasi-relaxation phases are

TABLE 1 Stages of the experiment.

Stage	Characteristic
1. Loading	Infinite fast ($\dot{\varepsilon}_{\parallel} \to \infty$)
2. Creeping	Approximately 3.5 h
3. Relaxation	Min 70, max 430 h ($\dot{\varepsilon}_{\parallel} \to 0$)
4. Unloading	Removing the specimen ($\dot{\varepsilon}_{\parallel} \to -\infty$)
5. Negative creeping	After removing ($\sigma = \dot{\sigma} = 0$)

ID: asme3b2server Time: 13:54 I Path: //chenas03/Cenpro/ApplicationFiles/Journals/ASTM/JTE#/Vol04504/160068/Comp/APPFile/AT-JTE#160068

managed separately. In all cases, the derivate values are obtained from fitted curves, and the parameters came from linear fitting.

CREEP

After the infinite fast loading, the creep phase lasted three and a half hours, and it is ended with putting blocks under the specimen's weighted end, the so-called "setup." The σ^d values versus experimental time were calculated from the previously introduced split. Then a curve was fitted to the gathered measurement points by the following equation:

$$y = y_0 + A_1 e^{\frac{-x}{\tau_1}} \tag{3}$$

In this uniaxial tensile test, the specimen was subjected to a strain over a long time, and the stress values were calculated over time. The resulting stress versus experimental time data could be fitted with the Prony series for tensile relaxation with the following equation [29]:

$$\sigma^d(t) = \sigma^d_\infty + \sum_{i=1}^{n} \sigma^d_i e^{\frac{-t}{\tau_i}} \tag{4}$$

where:

σ^d_∞ = the long-term modulus, and

τ_i = the relaxation times.

The data was fitted with the equation, and determining the necessary number of parameters for a good prediction was important. In this examination, only $i = 1$ for the creep phase was used, as can be seen in the equation above.

From the obtained curves, the stress derivatives were calculated. The same method was used to the deviatoric deformation (ε^d) values and the derivatives.

$$\varepsilon^d(t) = \varepsilon^d_\infty + \sum_{i=1}^{n} \varepsilon^d_i e^{\frac{-t}{\tau_i}} \tag{5}$$

where:

ε^d_∞ = the long-term modulus, and

τ_i = the relaxation times.

It should be noted that, here, the $i = 1$ value was used again; only one exponential provided appropriate results. The illustration of the fittings in the case of a specimen can be seen in **Fig. 3**.

The parameter values were obtained by linear fitting, and, as a result, it was found that in the creep phase besides the stress and deformation the use of their first derivative gives an accurate description. Therefore, during this period, higher derivatives are unnecessary in these experiments. The calculated parameter results for the two different aging series and for the unaged specimens can be seen in **Table 2**. Because of the degradation of PVC, τ^d and β^d values decrease and α^d values increase versus aging time.

For checking the appropriateness of the results, a corrected sample standard deviation (SD) was calculated for each specimen using the measured and computed ε^d values in the measurement points. The time and ε^d values and the calculated SD in the case of one sample specimen can be seen in **Table 3**. The values of SD for all specimens were between 0.0020 and 0.0031. **Fig. 4** shows the relationship between the measured points and the parameter results.

The characteristic parameter values determined during the creep period went under a significant change as the aging time increases. For modeling the creep, a Poynting–Thomson model proved to be adequate, as the second derivative's multiplication factor (γ^d) could be 0 and then the fitting still provides satisfactory results.

The results with the frequently used marking is shown by the following formula:

$$\tau^d = \tau, \quad \alpha^d = 2G, \quad \beta^d = 2\eta, \quad \gamma^d = \theta$$

Based on the marking above, the average values for the different aging times can be seen in **Table 4**.

QUASI-RELAXATION

The relaxation after the creep section began with the "setup" of the weighted end of the specimen. The length of the relaxation was not the same for every specimen, in some cases up to 430 h. Values obtained at the beginning of relaxation were not taken into account in the calculation because of the initial uncertainty. During relaxation, the longitudinal and transverse deformations were frozen, so the deformation was constant, and there is no need to take the derivatives into consideration. Therefore, only the deviatoric stress (σ^d) versus time points were used for fitting. In this case, one exponential was not sufficient; thus, two exponentials were used here (**Fig. 5**):

$$y = y_0 + A_1 e^{\frac{-x}{\tau_1}} + A_2 e^{\frac{-x}{\tau_2}} \tag{6}$$

As can be seen in **Fig. 5**, the one exponential fitting does not follow the changes in the early phase of the relaxation; therefore, two exponential approximations were applied in this case. This equation is similar to the previously introduced Prony series, with a value of $i = 2$:

$$\sigma^d(t) = \sigma^d_\infty + \sum_{i=1}^{n} \sigma^d_i e^{\frac{-t}{\tau_i}} = \sigma^d_\infty + \sigma^d_1 e^{\frac{-t}{\tau_1}} + \sigma^d_2 e^{\frac{-t}{\tau_2}} \tag{7}$$

where:

σ^d_∞ = the long-term modulus again, and

τ_i = the relaxation times.

Similarly to the creep part, the deviatoric stress derivatives were obtained from the curves. Then linear fitting was applied to determine the parameters; among them, the second derivatives were also necessary in this case. That means the previously introduced Kluitenberg–Verhás model is not appropriate for simulating the examined material's relaxation. The general

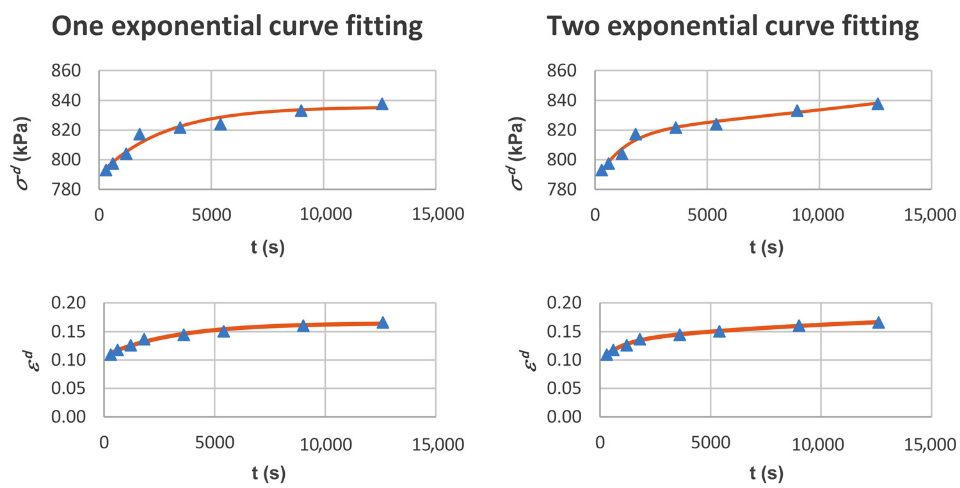

FIG. 3 One and two exponential curve fitting in the case of an aged specimen (aged2_2): R^2 values, one exponential 0.9467 (σ^d) and 0.9746 (ε^d); and two exponential 0.9566 (σ^d) and 0.9933 (ε^d).

equation has to be expanded with the second derivative of stress and its factor:

$$\sigma^d + \tau^d\dot{\sigma}^d + \xi^d\ddot{\sigma}^d = \alpha^d\varepsilon^d + \beta^d\dot{\varepsilon}^d + \gamma^d\ddot{\varepsilon}^d \qquad (8)$$

It should be noted that, in the creep period, only the first derivative of deformation and stress was taken into account. But here, a second derivative of stress was also necessary for appropriate characterization. The second derivative's multiplication coefficient (ξ^d) is called inertial factor using the analogy of the differential equation of vibration. The application of the second derivative occurred in other models, such as the Burgers model. The obtained equation modifies the Burgers model where the zero-order derivate of epsilon is not included. Therefore, this model can be called a modified Burgers model. The calculated parameters can be seen in **Table 5**. Because of the degradation of PVC, τ^d and ξ^d values decrease and α^d values increase versus aging time.

SD values were also calculated for checking the results of relaxation, but this time for the measured and calculated σ^d.

TABLE 2 Calculated parameters for creep section.

Aging Time (h)	Specimen	τ^d (h)	α^d (MPa)	β^d (MPa-h)
0	01	0.99	4.51	3.93
	02	1.65	4.48	4.63
	03	1.50	4.30	4.15
	Average	1.38	4.43	4.24
2541	Aged1_1	0.66	5.00	3.16
	Aged1_2	1.17	4.58	4.05
	Aged1_3	0.95	4.40	4.52
	Average	0.93	4.66	3.91
4000	Aged2_1	0.29	5.90	3.52
	Aged2_2	0.80	5.06	4.57
	Aged2_3	0.52	5.13	3.35
	Average	0.54	5.36	3.81

The SD for one sample specimen can be seen in **Table 6**, and in every case SD values were between 3.7670 and 6.7958. **Fig. 6** shows the connection between the measurement points and the calculated results.

In the case of relaxation, the determination of parameters were always performed for the same interval (24,000–250,000 s). But as seen in **Fig. 6**, the obtained parameter values well characterize the overall relaxation. The obtained fitted parameters are stable over the whole range. The results in the previously introduced form is shown in **Table 7**.

Conclusions

In these experiments, long-term tensile and quasi-relaxation tests were carried out on PVC fibers artificially aged by UV light for different aging times. During the evaluation of the measurement results, the creep and relaxation properties of the same material were examined separately. The parameters were determined by fitting for the deviatoric parts of the stress tensor and the deformation tensor. It was found for the creep phase that, in the examined case, the changes can be described by the

TABLE 3 Calculated SD for a specimen (aged1_1).

t (s)	Measurement ε^d Values	Model ε^d Values
300	0.1276	0.1323
660	0.1405	0.1378
1620	0.1480	0.1454
1800	0.1512	0.1507
3600	0.1592	0.1618
5400	0.1651	0.1669
9000	0.1713	0.1704
12,600	0.1727	0.1711
SD	0.0027	

FIG. 4 Calculated curves from the determined parameters and the measurement points (creep) min, R^2 0.9628.

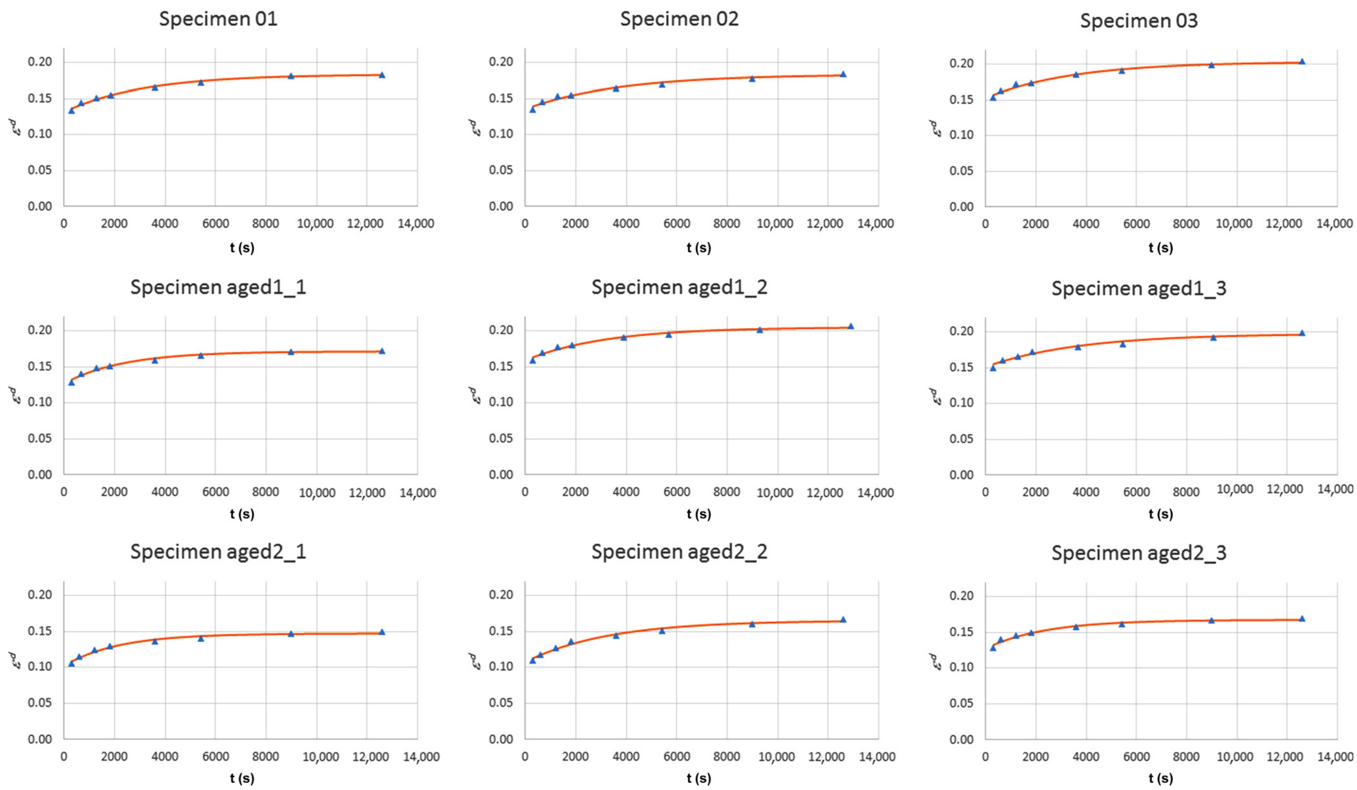

TABLE 4 Calculated average parameter values for creep section.

Aging Time (h)	τ (h)	G (MPa)	η (MPah)
0	1.38	2.22	2.12
2541	0.93	2.33	1.95
4000	0.54	2.68	1.95

Poynting–Thomson model, and the resulting parameter values well characterize the aging.

During the examination of relaxation, it was found that using the second derivatives are also necessary for the sufficiently accurate determination of stable parameters. Thus, in this case, a modified Burgers model was applied, and the

FIG. 5 One and two exponential curve fitting with zooming in on their first part (specimen aged2_2): R^2 values, one exponential 0.9625; and two exponential 0.9933.

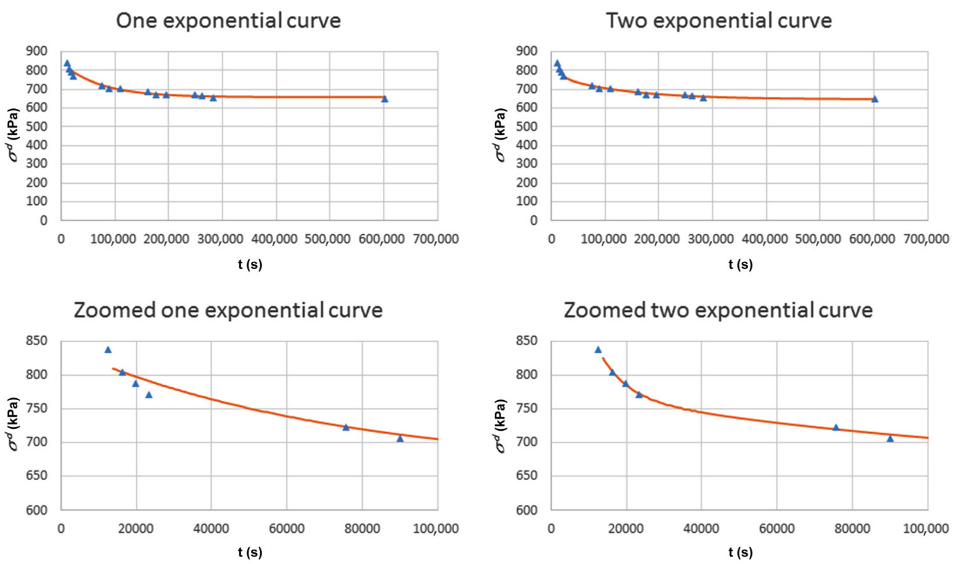

J_ID: JTE DOI: 10.1520/JTE20150186 Date: 21-June-16 Stage: Page: 7 Total Pages: 11

PROOF COPY [JTE20150186]

TABLE 5 Calculated parameters for quasi-relaxation section.

Aging Time (h)	Specimen	τ^d (h)	ξ^d (h^2)	α^d (MPa)
0	01	70.32	327.82	3.07
	02	168.89	742.49	2.63
	03	192.40	706.29	2.76
	Average	143.87	592.20	2.82
2541	Aged1_1	129.63	848.30	3.24
	Aged1_2	80.09	328.13	3.10
	Aged1_3	92.54	525.50	3.14
	Average	100.75	567.31	3.16
4000	Aged2_1	36.80	67.70	4.50
	Aged2_2	37.37	71.77	3.89
	Aged2_3	32.30	37.07	3.85
	Average	35.49	58.85	4.08

TABLE 6 Calculated SD for a specimen (aged1_2).

t (s)	Measurement σ^d Values	Model σ^d Values
23,700	865.76	868.37
30,900	847.34	846.73
77,700	792.08	790.82
84,900	792.08	786.44
92,100	773.66	782.35
102,900	773.66	776.63
110,100	773.66	773.02
117,300	773.66	769.54
164,100	755.24	749.31
178,500	736.82	743.78
200,100	736.82	736.01
255,900	718.40	718.59
SD	4.5399	

FIG. 6 Calculated curves from the determined parameters and the measurement points (quasi-relaxation) min, R^2 0.9720.

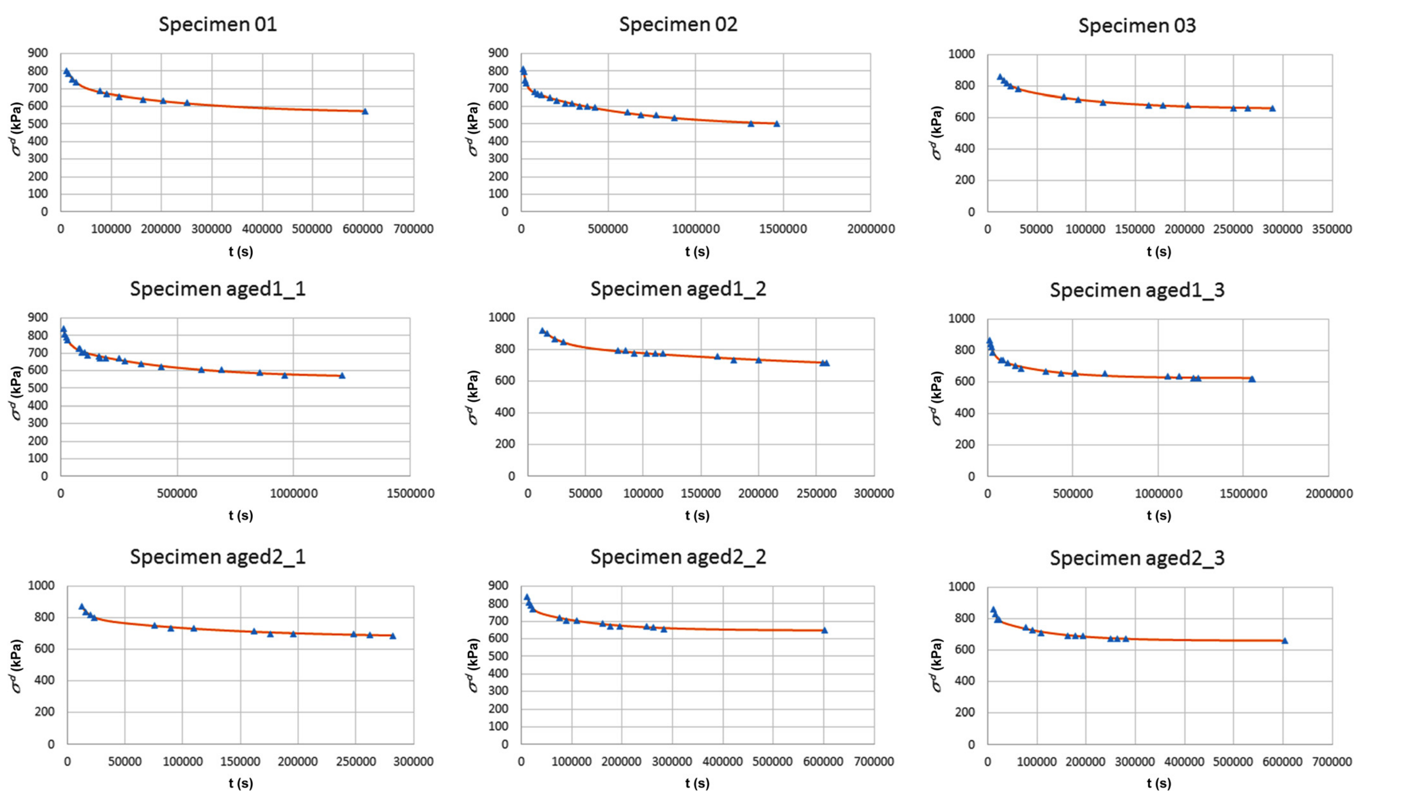

TABLE 7 Calculated average parameter values for quasi-relaxation section.

Aging Time (h)	τ (h)	ξ^d (h^2)	G (MPa)
0	143.87	592.20	1.41
2541	100.75	567.31	1.58
4000	35.49	58.85	2.04

resulting relaxation parameters are proven to be very stable and they well characterize the aging. Therefore, compared to other methods mentioned in the introduction, the applied method provides good results without fractional calculus or using a high number of parameters.

This work contributes to permanent literature by introducing a new, modified Burgers model for the relaxation behavior of PVC. The application of this model to other thermoplastic materials is possible. The calculated material parameter values of the examined material can be used for industrial applications.

Appendix

In the uniaxial tensile test, the total stress and deformation can be written as the following:

$$[\mathbf{S}] = \begin{pmatrix} \sigma & 0 & 0 \\ 0 & 0 & 0 \\ 0 & 0 & 0 \end{pmatrix} \quad \text{and} \quad [\mathbf{E}] = \begin{pmatrix} \varepsilon & 0 & 0 \\ 0 & \varepsilon_T & 0 \\ 0 & 0 & \varepsilon_T \end{pmatrix}$$

where:

ε = the longitudinal, and

ε_T = the transversal strain.

The stress tensor and deformation tensor can be split into deviatoric (marked with D) and spherical (or volumetric) parts (marked with V):

$$[\mathbf{S}^D] = \begin{pmatrix} \frac{2}{3}\sigma & 0 & 0 \\ 0 & -\frac{1}{3}\sigma & 0 \\ 0 & 0 & -\frac{1}{3}\sigma \end{pmatrix} = \begin{pmatrix} \sigma^D & 0 & 0 \\ 0 & -\frac{1}{2}\sigma^D & 0 \\ 0 & 0 & -\frac{1}{2}\sigma^D \end{pmatrix}$$

$$[\mathbf{S}^V] = \begin{pmatrix} \frac{1}{3}\sigma & 0 & 0 \\ 0 & \frac{1}{3}\sigma & 0 \\ 0 & 0 & \frac{1}{3}\sigma \end{pmatrix} = \frac{1}{3}\begin{pmatrix} \sigma^V & 0 & 0 \\ 0 & \sigma^V & 0 \\ 0 & 0 & \sigma^V \end{pmatrix}$$

$$[\mathbf{E}^D] = \begin{pmatrix} \frac{2}{3}(\varepsilon - \varepsilon_T) & 0 & 0 \\ 0 & -\frac{1}{3}(\varepsilon - \varepsilon_T) & 0 \\ 0 & 0 & -\frac{1}{3}(\varepsilon - \varepsilon_T) \end{pmatrix} = \begin{pmatrix} \varepsilon^D & 0 & 0 \\ 0 & -\frac{1}{2}\varepsilon^D & 0 \\ 0 & 0 & -\frac{1}{2}\varepsilon^D \end{pmatrix}$$

$$[\mathbf{E}^V] = \begin{pmatrix} \frac{1}{3}(\varepsilon + 2\varepsilon_T) & 0 & 0 \\ 0 & \frac{1}{3}(\varepsilon + 2\varepsilon_T) & 0 \\ 0 & 0 & \frac{1}{3}(\varepsilon + 2\varepsilon_T) \end{pmatrix} = \frac{1}{3}\begin{pmatrix} \varepsilon^V & 0 & 0 \\ 0 & \varepsilon^V & 0 \\ 0 & 0 & \varepsilon^V \end{pmatrix}$$

References

[1] Mahadevan, R. and Smith, L., "A Mechanistic Model Describing the Degradation of Polymers," *J. Polym. Environ.*, Vol. 15, No. 2, 2007, pp. 75–80.

[2] Pagnacco, E., Moreau, A., and Lemosse, D., "Inverse Strategies for the Identification of Elastic and Viscoelastic Material Parameters Using Full-Field Measurements," *Mater. Sci. Eng. A-Struct.*, Vol. 452, 2007, pp. 737–745. AQ3

[3] Atanackovic, T. M., "A Modified Zener Model of a Viscoelastic Body," *Continuum Mech. Therm.*, Vol. 14, No. 2, 2002, pp. 137–148.

[4] Haufe, A., Du Bois, P. A., Kolling, S., and Feucht, M., "A Semi-Analytical Model for Polymers Subjected to High Strain Rates," *5th European LS-DYNA Users Conference—Material Technology*, Birmingham, U.K., 2005, pp. 2b–58. AQ4

[5] Sahu, R., Patra, K., and Szpunar, J., "Experimental Study and Numerical Modelling of Creep and Stress Relaxation of Dielectric Elastomers," *Strain*, Vol. 51, No. 1, 2015, pp. 43–54.

[6] Krempl, E., and Ho, K., "An Overstress Model for Solid Polymer Deformation Behavior Applied to Nylon 66," *Time Dependent and Nonlinear Effects in Polymers and Composites, ASTM STP 1357*, R. A. Schapery, Ed., ASTM International, West Conshohocken, PA, 2000, pp. 118–137,

[7] Colak, O. U. and Dusunceli, N., "Modeling Viscoelastic and Viscoplastic Behavior of High Density Polyethylene (HDPE)," *J. Eng. Mater.*, Vol. 128, No. 4, 2006, pp. 572–578.

[8] Hartmann, S., "A Thermomechanically Consistent Constitutive Model for Polyoxymethylene—Experiments, Material Modelling and Computation," *Arch. Appl. Mech.*, Vol. 76, No. 5, 2006, pp. 349–366.

[9] Kästner, M., Blobel, S., Obst, M., Thielsch, K., and Ulbricht, V., "Experimental Characterization of the Visco-plastic Material Behaviour of Thermosets and Thermoplastics," *Appl. Mech. Mater.*, Vols. 24–25, 2010, pp. 195–200.

[10] Nikolov, S. and Doghri, I., "A Micro/Macro Constitutive Model for the Small-Deformation Behavior of Polyethylene," *Polymer*, Vol. 41, No. 5, 2000, pp. 1883–1891.

[11] Joseph, S. H., "A Method for Modelling the Nonlinear Viscoelastic Response of Polymers," *Mech. Time-Depend. Mater.*, Vol. 9, No. 1, 2005, pp. 35–69.

[12] Yonan, S. A., Soyarslan, C., Haupt, P., Kwiatkowski, L., and Tekkaya, A. E., "A Simple Finite Strain Non-Linear Visco-Plastic Model for Thermoplastics and Its Application to the Simulation of Incremental Cold Forming of Polyvinylchloride (PVC)," *Int. J. Mech. Sci.*, Vol. 66, 2013, pp. 192–201.

[13] Nonnenmacher, T. and Glöckle, W., "A Fractional Model for Mechanical Stress Relaxation," *Philos. Mag. Lett.*, Vol. 64, No. 2, 1991, pp. 89–93.

[14] Gloeckle, W. G. and Nonnenmacher, T. F., "Fractional Integral Operators and Fox Functions in the Theory of Viscoelasticity," *Macromolecules*, Vol. 24, 1991, pp. 6426–6434.

[15] Metzler, R. and Nonnenmacher, T. F., "Fractional Relaxation Processes and Fractional Rheological Models for the Description of a Class of Viscoelastic Materials," *Int. J. Plast.*, Vol. 19, 2003, pp. 941–959.

[16] Mainardi, F. and Spada, G., "Creep, Relaxation and Viscosity Properties for Basic Fractional Models in Rheology," *Eur. Phys. J. Special Topics*, Vol. 193, No. 1, 2011, pp. 133–160.

[17] Liu, J. G. and Xu, M. Y., "Higher-Order Fractional Constitutive Equations of Viscoelastic Materials Involving Three Different Parameters and Their Relaxation and Creep Functions," *Mech. Time-Depend. Mater.*, Vol. 10, No. 4, 2006, pp. 263–279.

[18] Jakubowicz, I., "Effects of Artificial and Natural Ageing on Impact-Modified Poly(Vinyl Chloride) (PVC)," *Polym. Test.*, Vol. 20, No. 5, 2001, pp. 545–551.

[19] Feldman, D., "Polymer Weathering: Photo-Oxidation," *J. Polym. Environ.*, Vol. 10, No. 4, 2002, pp. 163–173.

[20] Yarahmadi, N., Jakubowicz, I., and Hjertberg, T., "The Effects of Heat Treatment and Ageing on the Mechanical Properties of Rigid PVC," *Polym. Degrad. Stab.*, Vol. 82, No. 1, 2003, pp. 59–72.

[21] Zhou, Z. H., He, Y. L., Hu, H. J., Zhao, F., and Zhang, X. L., "Creep Performance of PVC Aged at Temperature Relatively Close to Glass Transition Temperature," *Appl. Math. Mech.-Engl.*, Vol. 33, No. 9, 2012, pp. 1129–1136.

[22] Barbero, E. J. and Ford, K. J., "Equivalent Time Temperature Model for Physical Aging and Temperature Effects on Polymer Creep and Relaxation," *J. Eng. Mater. Technol.*, Vol. 126, No. 4, 2004, pp. 413–419.

[23] Ito, M. and Nagai, K., "Analysis of Degradation Mechanism of Plasticized PVC Under Artificial Aging Conditions," *Polym. Degrad. Stabil.*, Vol. 92, No. 2, 2007, pp. 260–270.

[24] D'Aquino, C. A., Balmant, W., Ribeiro, R. L. L., Munaro, M., Vargas, J. V. C., and Amico, S. C., "A Simplified Mathematical Model to Predict PVC Photodegradation in Photobioreactors," *Polym. Test.*, Vol. 31, No. 5, 2012, pp. 638–644.

[25] Devasenapathi, V., Monish, P., and Prabu, S. B., "Experimental Investigation of Tensile Creep Behavior of Polymer Nanocomposites," *Int. J. Adv. Manuf. Tech.*, Vol. 44, No. 3, 2009, pp. 412–418.

[26] Ván, P., and Szarka, Z., "Rock Rheology—Time Dependence of Dilation and Stress Arround a Tunnel," *Eurock, 2006, Multiphysics Coupling and Long Term Behaviour in Rock Mechanics*, A. van Cotthem, R. Charlier, J. Thimus, and J. Tshibangu, Eds., Taylor & Francis, London, 2006, p. 357.

[27] Fülöp, T., and Béda, G., "Rheological Dynamics of Tunnels—An Analytical Investigation," *Rock Engineering in Difficult Ground Conditions: Soft Rocks and Karst*, I. Vrkljan, Ed., Taylor & Francis, London, 2010, p. 441.

[28] Asszonyi, C., Fülöp, T., and Ván, P., "Distinguished Rheological Models for Solids in the Framework of a Thermodynamical Internal Variable Theory," *Continuum Mech. Thermodyn.*, Vol. 27, No. 6, 2015, pp. 971–986.

[29] Barbero, E. J., *Finite Element Analysis of Composite Materials*, CRC, Boca Raton, FL, 2007.